Calpain is required for macroautophagy in mammalian cells

Francesca Demarchi,[1] Cosetta Bertoli,[1] Tamara Copetti,[1] Isei Tanida,[2] Claudio Brancolini,[3] Eeva-Liisa Eskelinen,[4] and Claudio Schneider[1,3]

[1]Laboratorio Nazionale Consorzio Interuniversitario Biotecnologie, 34012 Trieste, Italy
[2]Department of Biochemistry, Juntendo University School of Medicine, Bunkyo-ku, Tokyo 113-8421, Japan
[3]Dipartimento di Scienze e Tecnologie Biomediche, Universitá degli Studi di Udine, 33100 Udine, Italy
[4]Department of Biological and Environmental Sciences, Division of Biochemistry, 00014 University of Helsinki, Helsinki, Finland

Ubiquitously expressed micro- and millicalpain, which both require the calpain small 1 (CAPNS1) regulatory subunit for function, play important roles in numerous biological and pathological phenomena. We have previously shown that the product of GAS2, a gene specifically induced at growth arrest, is an inhibitor of millicalpain and that its overexpression sensitizes cells to apoptosis in a p53-dependent manner (Benetti, R., G. Del Sal, M. Monte, G. Paroni, C. Brancolini, and C. Schneider. 2001. *EMBO J.* 20:2702–2714). More recently, we have shown that calpain is also involved in nuclear factor κB activation and its relative prosurvival function in response to ceramide, in which calpain deficiency strengthens the proapoptotic effect of ceramide (Demarchi, F., C. Bertoli, P.A. Greer, and C. Schneider. 2005. *Cell Death Differ.* 12:512–522). Here, we further explore the involvement of calpain in the apoptotic switch and find that in calpain-deficient cells, autophagy is impaired with a resulting dramatic increase in apoptotic cell death. Immunostaining of the endogenous autophagosome marker LC3 and electron microscopy experiments demonstrate that autophagy is impaired in CAPNS1-deficient cells. Accordingly, the enhancement of lysosomal activity and long-lived protein degradation, which normally occur upon starvation, is also reduced. In CAPNS1-depleted cells, ectopic LC3 accumulates in early endosome-like vesicles that may represent a salvage pathway for protein degradation when autophagy is defective.

Introduction

Macroautophagy, which is usually referred to as autophagy, is responsible for degradation of the majority of intracellular proteins in mammalian cells, particularly during starvation-induced proteolysis. Cytosolic proteins, organelles, and selected regions of the nucleus can be cleared by autophagy to ensure cellular homeostasis and remove damaged or unwanted products (Klionsky, 2005). Cytoplasmic constituents are first enclosed by a double-membrane autophagosome; next, the outer membrane of the autophagosome fuses with the lysosome, with the consequent destruction of the cargo and the inner membrane of the autophagosome by hydrolytic enzymes.

The autophagic pathway has been dissected at the molecular level in yeast, in which 27 genes, referred to as *ATG*, have been found to be required for autophagosome formation (Klionsky and Ohsumi, 1999; Yorimitsu and Klionsky, 2005). Two ubiquitin-like conjugation systems are involved in the process: one mediates the covalent attachment of Atg12 to Atg5, and the other mediates the conjugation of Atg8 to phosphatidylethanolamine (Ichimura et al., 2000). The resulting products, Atg12–Atg5 and Atg8-phosphatidylethanolamine, are essential for proper autophagosome formation. Only a small fraction of the Atg12–Atg5 complex localizes at the autophagic isolation membrane throughout elongation, and the complex dissociates when the phagosome is complete. On the other hand, Atg8 remains on the mature autophagosome constituting the recognized consensus marker of this structure. These two conjugation systems are highly conserved in mammalian cells. *ATG5*-deficient stem cells have been instrumental for demonstrating that the Atg12–Atg5 complex localizes at autophagosome precursors and plays an essential role in autophagosome formation (Mizushima et al., 2001). The production of *ATG5*-deficient mice has revealed that autophagy is required for neonatal

Correspondence to Claudio Schneider: schneide@lncib.it

Abbreviations used in this paper: 3MA, 3-methyladenine; AV, autophagic vacuole; CAPNS, calpain small; EBSS, Earle's balanced salt solution; MEF, mouse embryonic fibroblast; PI, propidium iodide.

The online version of this article contains supplemental material.

The Journal of Cell Biology, Vol. 175, No. 4, November 20, 2006 595–605
http://www.jcb.org/cgi/doi/10.1083/jcb.200601024

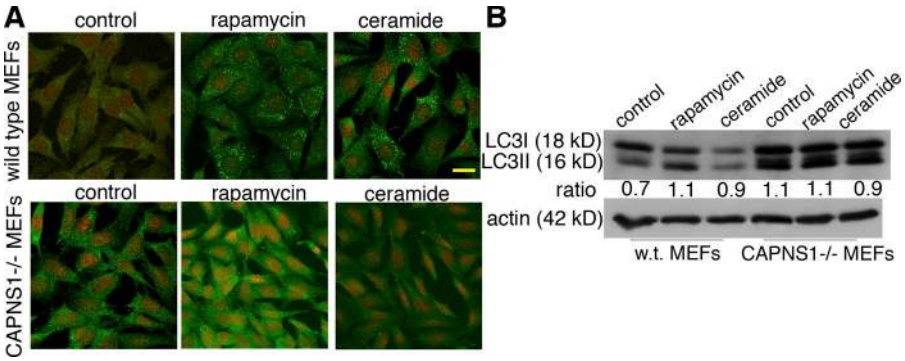

Figure 1. **CAPNS1$^{-/-}$ MEFs lacking calpain activity are defective in autophagosome formation.** (A and B) Wild-type and CAPNS1$^{-/-}$ MEFs were stimulated for 3 h with rapamycin or ceramide and analyzed by immunofluorescence using an anti-LC3–specific antibody and PI to stain nuclei (A) or were lysed and used for Western blot analysis with the same antibody to detect both cytoplasmic LC3I and membrane-associated LC3II (B). Actin was used as a loading control. (B) The ratio between the intensities of LC3II and LC3I bands is indicated below each lane. Bar, 20 μm.

survival before maternal feeding (Kuma et al., 2004). The analysis of endogenous LC3, which is one of the mammalian homologues of Atg8, and the production of transgenic mice expressing a fluorescent autophagosomal LC3 have shown that the regulation of autophagy is organ dependent and that the role of autophagy is not restricted to the starvation response (Mizushima et al., 2004).

A pivotal role for autophagy in growth control has emerged from studies on Beclin1, the mammalian homologue of *ATG6*. The Beclin1 gene is deleted in several types of breast cancer that are unable to activate autophagy (Liang et al., 1999) and functions as a haploinsufficient tumor suppressor gene (Yue et al., 2003). In addition to involvement in growth control, programmed autophagy plays a role in differentiation (Ghidoni et al., 1996; Lee et al., 2002) and tissue remodeling (Rusten et al., 2004). Moreover, autophagy may be artificially induced by radiation and treatment with certain drugs, including rapamycin (Noda and Ohsumi, 1998), ceramide (Scarlatti et al., 2004), arsenic trioxide (Kanzawa et al., 2003), and tamoxifen (Bursch et al., 2000); the final outcome of such induction is still a matter of debate (Kroemer and Jaattela, 2005).

The calpain family of cysteine proteases is composed of both ubiquitous and tissue-specific isoforms that share homology in their protease domain and are calcium dependent (Goll et al., 2003). The best-characterized ubiquitous calpains are the isoforms μ- and m-calpain, which are also known as calpain 1 and calpain 2, respectively. Both contain an 80-kD catalytic subunit and share a common 28-kD regulatory subunit commonly known as calpain 4 that is required for proper activity. Hereafter, calpain 4 will be referred to as calpain small 1 (CAPNS1) in accordance with the nomenclature reported at the calpain website (http://ag.arizona.edu/calpains). A homologue to CAPNS1, CAPNS2, has been described previously (Schad et al., 2002). This protein appears to be a functional equivalent to CAPNS1 in vitro; however, its in vivo function and tissue distribution are still controversial. Interestingly, ubiquitous calpains are associated with the endoplasmic reticulum and Golgi, a likely reservoir for autophagosome membranes (Hood et al., 2004), where the essential autophagy regulatory complex PI3K–Beclin also localizes (Kihara et al., 2001).

Calpain is required for normal embryonic development. Indeed, the targeted disruption of CAPNS1 is embryonic lethal at days 10 and 11 as a result of severe defects in vascular development (Arthur et al., 2000). Calpain is a regulator of adhesive complex dynamics in adherent cells (Bhatt et al., 2002); it plays an important role in osteoclastic bone resorption (Hayashi et al., 2005) and is required for phagocytosis in human neutrophils (Dewitt and Hallett, 2002).

We have become interested in calpain function because of our observation that the product of GAS2, a gene specifically induced at growth arrest, is in fact an inhibitor of millicalpain and that its overexpression sensitizes cells to apoptosis in a p53-dependent manner (Benetti et al., 2001). More recently, we have shown that calpain is also involved in NF-κB activation and in its relative prosurvival function in response to ceramide, in which calpain deficiency strengthens the proapoptotic effect of ceramide (Demarchi et al., 2005). In this study, we further explore the involvement of calpain in the apoptotic switch and find that in calpain-deficient cells, autophagy is impaired with a resulting dramatic increase in apoptotic cell death.

Results

The lack of calpain activity is coupled to a block in autophagy

We have previously reported that calpain plays a crucial role in cell death regulation in response to ceramide. Indeed, we demonstrated that the lack of calpain activity results in a considerable

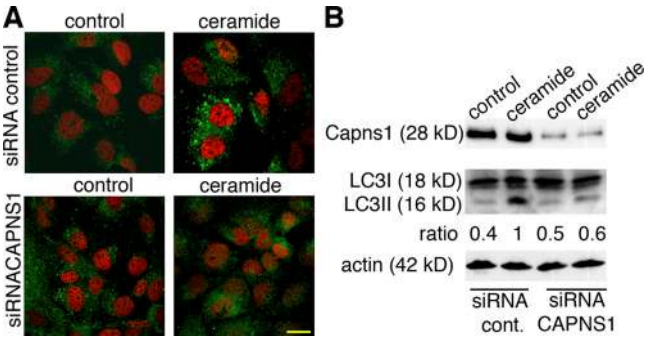

Figure 2. **CAPNS1 depletion is coupled to a block in autophagosome formation in human cells.** (A and B) U2OS cells were silenced with control siRNA or CAPNS1 siRNA and, 72 h later, were stimulated with ceramide for 3 h to trigger macroautophagy, as indicated in the figure. Afterward, the cells were fixed and decorated with anti-LC3 and PI (A) or were lysed to perform Western analysis against endogenous LC3 (B). Actin was used as a loading control; anti-CAPNS1 antibody was used to check silencing efficiency. (B) The ratio between the intensities of LC3II and LC3I bands is indicated below each lane. Bar, 20 μm.

increase in apoptotic cell death (Demarchi et al., 2005). To further investigate the involvement of calpain in the modulation of alternative types of cell death, in this study, we address the role of calpain in autophagy. LC3 is the only available specific marker to detect autophagosomes in mammalian cells (Kabeya et al., 2000).

To directly tackle the question of whether calpain is required in autophagy, we analyzed endogenous LC3 in response to ceramide and rapamycin by means of immunofluorescence in wild-type and CAPNS1$^{-/-}$ mouse embryonic fibroblasts (MEFs). CAPNS1$^{-/-}$ MEFs, which are also known as calpain 4$^{-/-}$ MEFs, were derived from CAPNS1 (calpain 4) knockout mice and were shown to lack calpain activity (Arthur et al., 2000). Wild-type and CAPNS1$^{-/-}$ MEFs were induced with each stimulus for 3 h or were left untreated. Afterward, the cells were fixed and subjected to immunofluorescence analysis with an anti-LC3 antibody. As shown in Fig. 1 A (top), wild-type MEFs are faintly labeled by anti-LC3 antibody and show a clear induction of autophagosome formation after rapamycin or ceramide treatment. On the other hand, CAPNS1$^{-/-}$ MEFs show a higher diffuse background that does not substantially vary after stimulation with rapamycin or ceramide (Fig. 1 A, bottom).

In a parallel experiment, rapamycin and ceramide were used to stimulate wild-type and CAPNS1$^{-/-}$ MEFs, and the lysates were analyzed by Western blotting to detect both cytoplasmic LC3-I and its proteolytic derivative LC3-II that preferentially associates with autophagosomal membranes (Kabeya et al., 2004). In agreement with the immunofluorescence data, both rapamycin and ceramide trigger an increase of LC3II with respect to LC3I in wild-type cells, whereas the ratio between the two LC3 forms is not considerably altered by both stimuli in CAPNS1$^{-/-}$ MEFs (Fig. 1 B).

The fate of endogenous LC3 upon autophagy induction was also addressed in human U2OS cells. U2OS cells were transfected with a scrambled siRNA (siRNA control) or with a CAPNS1-specific siRNA. 72 h later, autophagy was induced by a 3-h incubation with ceramide, and the cells were either fixed and analyzed by immunofluorescence or lysed and subjected to Western blot analysis. As shown in Fig. 2 A, CAPNS1 depletion prevents the formation of bona-fide autophagosomes upon induction with ceramide. Accordingly, the increase in the endogenous membrane-bound LC3II after ceramide treatment is clearly defective after CAPNS1 silencing (Fig. 2 B).

Calpain-deficient cells show a defect in lysosomal activation and long-lived protein degradation

To further assess the requirement of calpain for the autophagic process, we followed the increase of lysosomal activity occurring

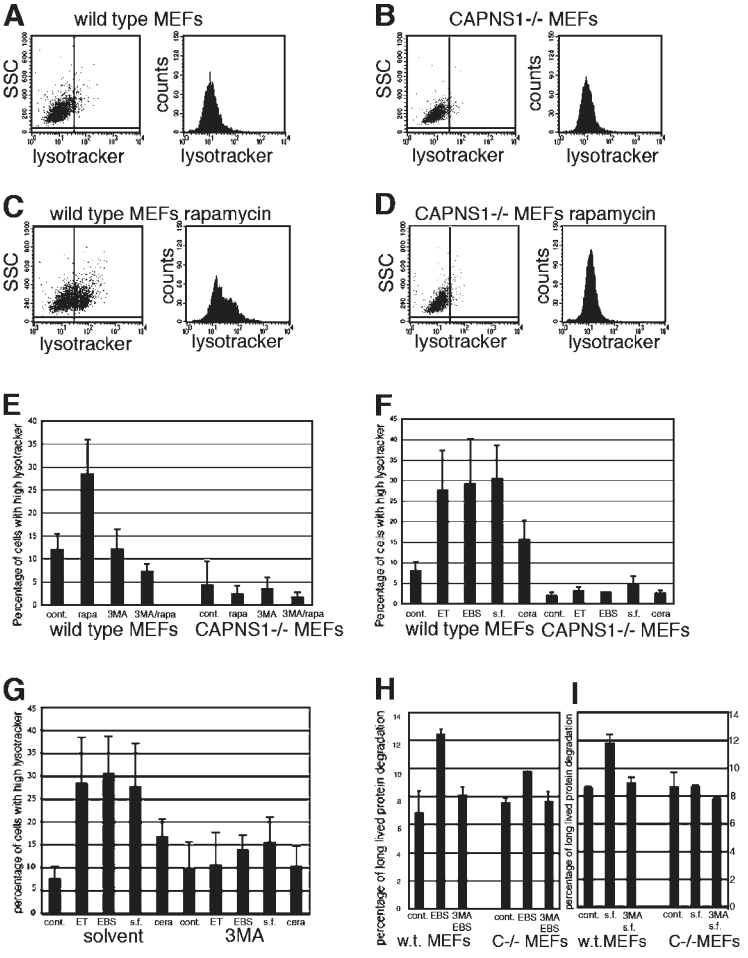

Figure 3. **Lysosomal induction and long-lived protein degradation are hampered in CAPNS1-deficient MEFs.** Wild-type and CAPNS1 MEFs were incubated with the stimuli indicated, namely rapamycin (rapa), etoposide (ET), EBSS (EBS), serum-free medium (sf), and ceramide (cera), in the presence or absence of 3MA and were trypsinized, stained with LysoTracker green, and analyzed by FACS. (A–D) Representative FACS profiles obtained after LysoTracker staining of wild-type and CAPNS1$^{-/-}$ MEFs before and after rapamycin treatment. The gate set between 10^1 and 10^2 separates the cells with high fluorescence from the background population. (E–G) The histograms report the percentage of cells with high LysoTracker staining and represent the mean values obtained in four independent experiments. (H and I) Wild-type and CAPNS1$^{-/-}$ MEFs were grown for 4 h in amino acid–free medium (H) or in serum-free medium (I) in the presence or absence of the autophagy inhibitor 3MA, and, subsequently, long-lived protein degradation was scored as the percentage of TCA-soluble counts on total radioactivity in a standard protein degradation assay. The histograms report the mean values obtained in four independent experiments. Error bars represent SD. SSC, side scatter.

after autophagy induction by means of LysoTracker staining and FACS analysis. Wild-type and CAPNS1$^{-/-}$ MEFs were incubated with rapamycin for 24 h, trypsinized, stained with LysoTracker green, and analyzed by FACS. The results obtained in a typical experiment are reported in Fig. 3 (A–D). A net increase in the percentage of cells that are highly labeled with LysoTracker occurs after rapamycin treatment of wild-type MEFs (Fig. 3 C) as compared with control untreated cells (Fig. 3 A), clearly showing that rapamycin results in an increase in lysosomal activity. On the contrary, in CAPNS1$^{-/-}$ MEFs, rapamycin is ineffective in inducing an increase in LysoTracker fluorescence intensity (Fig. 3, compare B with D). The mean values of the percentage of cells highly labeled by LysoTracker obtained in four independent experiments are reported in Fig. 3 E. To determine whether the increase in lysosomal activity was dependent on macroautophagy induction, 3-methyladenine (3MA) was added just before stimulation with rapamycin. 3MA clearly inhibits the increase in LysoTracker staining, indicating the specificity of the induction (Fig. 3 E). Next, other autophagic stimuli, namely etoposide, starvation in Earle's balanced salt solution (EBSS) or serum-free medium, and ceramide, were used to induce autophagy in wild-type and CAPNS1$^{-/-}$ MEFs using the same type of assay. As shown in Fig. 3 F, all four stimuli induce autophagy-dependent lysosomal activation after 3 h in wild-type MEFs but not in CAPNS1$^{-/-}$ MEFs; moreover, the increase in LysoTracker labeling is dramatically reduced upon the addition of 3MA just before induction (Fig. 3 G).

To further investigate the requirement of calpain in autophagy, we monitored long-lived protein degradation upon amino acid starvation both in wild-type and CAPNS1$^{-/-}$ MEFs according to standard protocols (Pattingre et al., 2003). Amino acid starvation induces an increase in bulk protein degradation in both cell lines. However, such an increase is considerably lower in calpain-deficient cells as compared with wild-type cells (Fig. 3 H). A reduction in protein degradation occurs in the presence of the inhibitor 3MA in both cell lines, indicating that although considerably reduced, autophagy may still occur in CAPNS1$^{-/-}$ MEFs as a consequence of amino acid starvation. Alternatively, this result might be caused by an effect of 3MA on alternative degradation pathways, as a similar effect is also observed in autophagy-defective *ATG5*$^{-/-}$ cells (Mizushima et al., 2001). Similar results were obtained by studying long-lived protein degradation upon serum starvation (Fig. 3 I), confirming the importance of calpain in activating protein degradation through the autophagic process.

Calpain is required for autophagosome formation in response to rapamycin

Electron microscopy was used to directly analyze and quantify autophagosomes in wild-type and CAPNS1$^{-/-}$ MEFs grown in control serum-containing medium and after autophagy induction with rapamycin or amino acid–free medium (EBSS). The morphology of early autophagic vacuole (AV [AVi]) and late AV (AVd) profiles of wild-type MEFs are shown in Fig. 4 (A and B, respectively). The quantitative results obtained are represented in Fig. 4 C.

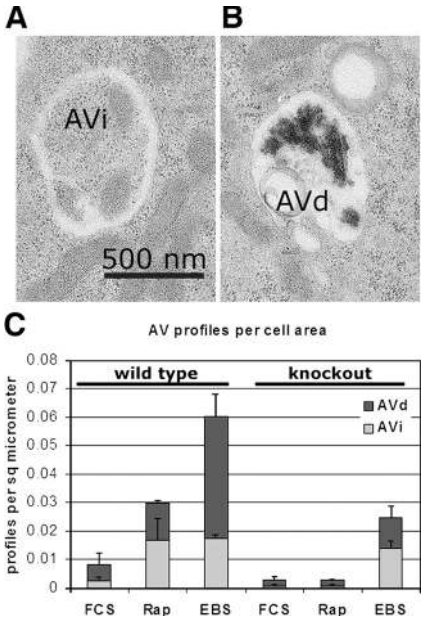

Figure 4. **Autophagosome formation is hampered in CAPNS1$^{-/-}$ MEFs.** (A and B) The electron micrographs show the ultrastructure of early (A) and late autophagosomes (B) in wild-type MEFs. The cell area on the grid squares was estimated by point counting using negatives taken at 600×. (C) Quantification of autophagosomes in wild-type and CAPNS1$^{-/-}$ MEFs (knockout) grown in control serum-containing medium (FCS) or induced for 3 h with EBSS (EBS) or rapamycin (Rap). Error bars indicate the SEM. The number of AVi and AVd profiles was counted under the microscope at 12,000× from four to five grid squares for each sample.

These electron microscopy experiments demonstrate that in CAPNS1$^{-/-}$ MEFs, autophagosome formation is completely abolished in response to rapamycin. In the case of EBSS-induced autophagy, CAPNS1$^{-/-}$ MEFs do show autophagosome formation but at a substantially reduced level compared with wild-type MEFs. In this last case, as shown in Fig. S2 (available at http://www.jcb.org/cgi/content/full/jcb.200601024/DC1), the morphology of the autophagosomes is not altered in CAPNS1$^{-/-}$ MEFs with respect to wild-type MEFs. This led us to conclude that the mechanics of autophagosome formation are still functional in CAPNS1$^{-/-}$ MEFs, however severely impaired in their efficiency. The diminished accumulation of autophagosomes in CAPNS1$^{-/-}$ MEFs maintained in EBSS medium may therefore suggest that the dramatic reprogramming of cell functions occurring upon amino acid deprivation may also involve the activation of some autophagic pathways not strictly requiring calpain function. Alternatively, because EBSS possibly represents a stronger and broader stimulus in respect to rapamycin, residual calpain activity caused by some other calpain isoforms may be sufficient to trigger autophagy, albeit at a reduced level.

This evidence prompted us to monitor Tor activity in both cell lines before and after rapamycin treatment using S6 kinase phosphorylation as readout. The results shown in Fig. S3 (available at http://www.jcb.org/cgi/content/full/jcb.200601024/DC1) clearly indicate that Tor is active in both cell lines, where it is inhibited with similar efficiency upon rapamycin addition.

Further studies are required to define the key regulatory elements targeted by calpain for the efficient induction of autophagosome formation.

Ectopic LC3 constitutively forms discrete bodies in calpain-deficient MEFs

A widely used method to study autophagy is monitoring the redistribution of the overexpressed autophagosome marker LC3 from a mostly diffused localization to a punctuated pattern upon the addition of an autophagic stimulus. Therefore, in parallel to the studies on endogenous LC3, we monitored autophagosome formation after overexpressed GFP-LC3 localization in wild-type and CAPNS1$^{-/-}$ MEFs. 16 h after transfection, the cells were preincubated with the macroautophagy inhibitor 3MA or solvent alone, and ceramide was added for 3 h to induce autophagy (Scarlatti et al., 2004). The cells were subsequently fixed to analyze overexpressed LC3 by fluorescence microscopy. As shown in Fig. 5 A, in wild-type MEFs, LC3 produces a mostly diffuse staining in the absence of stimulus and after 3MA treatment. After induction with ceramide, LC3 accumulates in the autophagosomes, whose formation is prevented by 3MA pretreatment, indicating the specificity of autophagy induction. However, in CAPNS1$^{-/-}$ MEFs, LC3 accumulates in specific bodies even under basal conditions; incubation with the autophagy inhibitor 3MA in this case does not prevent the formation of LC3 spots. In addition, the number of cells with intensely stained bodies does not substantially increase after the addition of ceramide (Fig. 5 B). Each experiment was repeated at least four times, obtaining reproducible results. For each experiment, the percentage of cells with LC3 bodies was counted, and the mean value ± SD is reported in the figure. At least 200 cells were analyzed for each independent experiment.

To further monitor autophagy induction, wild-type and CAPNS1$^{-/-}$ MEFs overexpressing GFP-LC3 were challenged with several stimuli that were previously used to induce autophagy, namely rapamycin (Noda and Ohsumi, 1998), amino acid–free medium (Neely et al., 1977), serum starvation (Pfeifer, 1973), and etoposide (Shimizu et al., 2004). All of the treatments triggered autophagosome formation in wild-type MEFs (Fig. 5 C) while leaving unchanged the LC3 staining pattern in CAPNS1$^{-/-}$ MEFs (not depicted). Altogether, these results further suggest that autophagy is impaired in cells lacking calpain activity, where overexpressed LC3 constitutively accumulates into specific bodies.

Calpain silencing is coupled to the accumulation of overexpressed LC3 in human cells

To verify whether the constitutive accumulation of ectopic LC3 into the observed specific bodies in CAPNS1$^{-/-}$ MEFs was a peculiarity of the cell line used or a consequence of calpain inactivation, we monitored the effect of calpain silencing by siRNA on autophagosome formation in the human osteosarcoma cell line U2OS. An *ATG5*-specific siRNA that has been previously described (Boya et al., 2005) was used as a tool to prevent autophagy, allowing the distinction between true autophagosomes

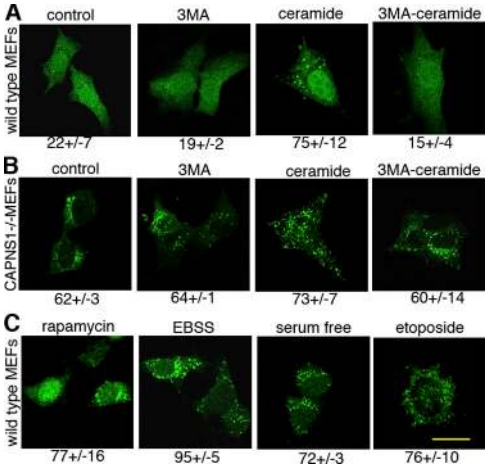

Figure 5. **Ectopic LC3 constitutively accumulates in vesicles in CAPNS1$^{-/-}$ MEFs.** (A–C) Wild-type (A and C) and CAPNS1$^{-/-}$ MEFs (B) were transfected with GFP-rLC3, and, 16 h later, the cells were treated for 3 h with the stimuli indicated. Afterward, the cells were fixed and analyzed by fluorescence microscopy. Representative fields are shown. The different patterns of GFP-LC3 distribution were scored in 250 transfected cells for at least three independent experiments. The mean of the percentage of cells with intensely stained bodies and relative SD are indicated beneath each image. Bar, 20 μm.

and other undefined structures containing ectopic LC3. U2OS cells were transfected with a scrambled siRNA (siRNA control) or with a CAPNS1-specific siRNA in combination with *ATG5* siRNA or an ineffective siRNA as a control.

48 h later, the cells were transfected with GFP-LC3, and, after an additional 16 h, autophagy was induced by a 3-h incubation with ceramide. The fixed cells were finally analyzed by fluorescence microscopy. As shown in Fig. 6 A, LC3 appears diffuse in control U2OS cells and, after induction with ceramide, becomes associated with autophagosomes, which are not formed by specifically inhibiting autophagy through *ATG5* siRNA. On the other hand, CAPNS1-silenced U2OS cells show LC3-positive bodies in the absence of stimulation, and the distribution of GFP-LC3 is not altered by *ATG5* silencing. In addition, the LC3 staining pattern is not considerably affected by ceramide (Fig. 6 B).

To mark and analyze the LC3 pattern specifically in the cells where CAPNS1 is silenced, we developed an siCAPNS1-GFP p-superior plasmid (siCAPNS1-GFP) allowing the simultaneous expression of CAPNS1 siRNA and GFP. In parallel, we produced a U2OS-derivative cell line expressing HcRed-LC3 (U2OS-LC3) as a tool to study autophagy induction. U2OS-LC3 cells were transfected with a control vector (sicontrol-GFP) or with siCAPNS1-GFP plasmid; after 48 h, they were stimulated or left unstimulated with ceramide for 3 h and were fixed and analyzed by fluorescence microscopy.

As shown in Fig. 6 C, in the cells transfected with the control plasmid, HcRed-LC3 appears diffuse before induction and forms autophagosomes after ceramide treatment as expected. However, siCAPNS1-GFP–transfected cells show a punctuated LC3 pattern both in the presence and absence of ceramide stimulation. Collectively, the data obtained in U2OS cells are in agreement with the data obtained comparing wild-type

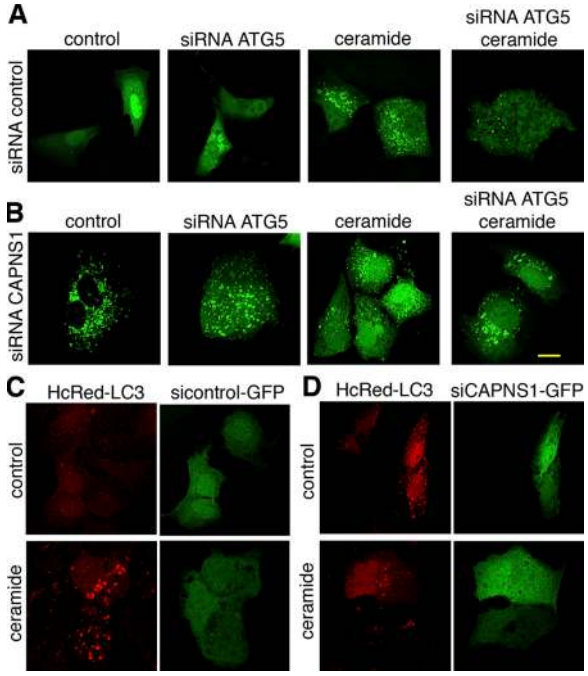

Figure 6. **Ectopic LC3 forms specific bodies in CAPNS1-depleted human cells.** (A and B) U2OS cells were silenced with a control siRNA (A) or with a CAPNS1 siRNA (B) in combination with a control siRNA or *ATG5* siRNA as indicated. After 48 h, the cells were transfected with GFP-hLC3 and, 16 h later, were incubated for 3 h with ceramide or solvent alone as a negative control. They were subsequently fixed and analyzed by fluorescence microscopy. Representative fields are shown. (C and D) A U2OS-derivative cell line stably expressing HcRed-hLC3 (U2OS-LC3) was established. U2OS-LC3 cells were transfected with si-control-GFP (C) or siCAPNS1-GFP (D) expression vectors and, 48 h later, were either treated with ceramide or with solvent alone for 3 h as indicated. Finally, the cells were fixed and analyzed by fluorescence microscopy. The different patterns of GFP-LC3 distribution were scored in 250 transfected cells for at least three independent experiments. Bar, 20 μm.

with CAPNS1$^{-/-}$ MEFs, demonstrating that in CAPNS1-depleted cells, overexpressed LC3 accumulates in specific bodies independently of autophagy induction.

Ectopic LC3 bodies constitutively present in CAPNS1-depleted cells are enriched in endosome markers

To investigate the identity of LC3-containing structures in CAPNS1-depleted cells, we analyzed whether overexpressed LC3 would eventually colocalize with specific endosomal markers both in control and in CAPNS1-silenced U2OS-LC3 cells. 48 h after silencing with control or CAPNS1 siRNA, autophagy was induced by ceramide together with pepstatin to inhibit lysosomal activity and freeze any eventual transient colocalization event. Thereafter, the cells were fixed and subjected to immunofluorescence against the markers LAMP-2, EEA1, and transferrin receptor and were analyzed by a confocal microscope. Representative images are shown in Fig. 7. The colocalization of LC3 with the endosomal markers was quantified using ImageJ software (colocalizer plug-in). The Pearson correlation coefficient (R) is reported near each merged image. Altogether, the data indicate that overexpressed LC3 bodies are enriched in endosome markers specifically in calpain-depleted cells.

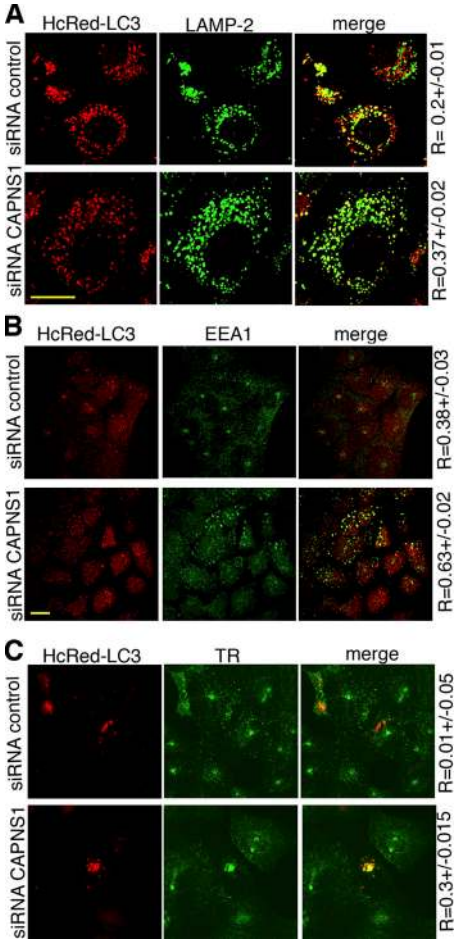

Figure 7. **Ectopic LC3 bodies are enriched with endosome markers in CAPNS1-depleted cells.** (A–C) U2OS-LC3 cells were silenced with a control siRNA or a CAPNS1 siRNA as indicated and, 48 h later, were stimulated for 3 h with ceramide to induce macroautophagy. Pepstatin A was added to inhibit lysosomal activity and freeze any colocalization event between LC3 vesicles and lysosomes. Subsequently, the cells were fixed, decorated with anti–LAMP-2 (A), anti-EEA1 (B), and antitransferrin receptor (TR; C), and analyzed by confocal microscopy. Images of representative fields were taken. The Pearson's correlation coefficient, R, is reported for each merge image. Bars, 20 μm.

To precisely define the identity of the LC3-positive bodies that accumulate in calpain-deficient cells, immunoelectron microcopy studies were performed. U2OS cells were transfected with GFP-LC3 and siRNA specific for CAPNS1 as described in the first section of Results and were fixed in PFA. Double labeling with GFP and LAMP-2 antibodies allowed us to detect GFP-LC3 bodies and also mark endosomes in the same experiment. As expected, GFP-LC3 partly accumulates in specific bodies, as shown in Fig. 8 (A and B). The gold particles indicating the presence of GFP-LC3 bodies (Fig. 8, large gold dots) were associated with endosome-like structures, some of which were also positive for LAMP-2 (Fig. 8; small gold dots are indicated by arrowheads). The morphology and LAMP-2 labeling pattern of GFP-LC3 structures corresponded to that of early endosome-like vesicles, clearly confirming that GFP-LC3 bodies accumulating in CAPNS1-depleted cells are not autophagosomes.

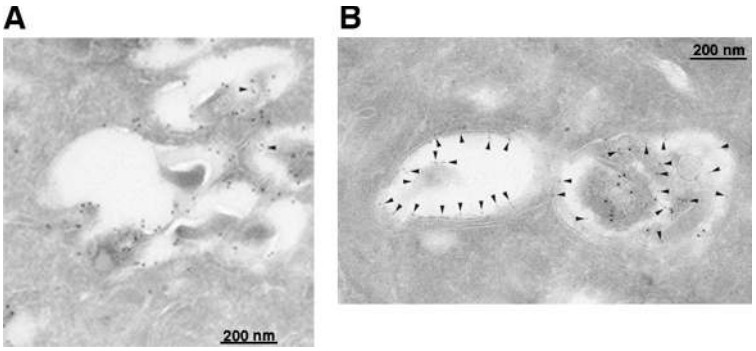

Figure 8. **GFP-LC3 bodies in CAPNS1-depleted cells are endosome-like structures.** Representative immunoelectron microscopy microphotographs showing the ultrastructure of GFP-LC3 bodies in CAPNS1-depleted U2OS cells. Large gold dots mark GFP-positive structures, whereas small gold dots (indicated by arrowheads) are labeled with anti–LAMP-2.

The calpain-dependent impairment of autophagy sensitizes cells to apoptosis

We have previously reported that ceramide triggers apoptosis and induces an NF-κB–dependent prosurvival pathway through calpain. Accordingly, in calpain-deficient cells, apoptosis is enhanced (Demarchi et al., 2005). In this study, we have demonstrated that calpain is required to induce autophagy in response to ceramide, etoposide, and amino acid or serum starvation. Recent studies indicate the existence of a negative cross-regulation between autophagy and apoptosis (Yu et al., 2004; Boya et al., 2005; Takacs-Vellai et al., 2005). However, there are examples of a mutual requirement between the two pathways (Camougrand et al., 2003; Martin and Baehrecke, 2004). Therefore, we decided to define the effect of the calpain-related autophagy block on apoptosis induction in the cellular systems used for this study.

Wild-type and CAPNS1$^{-/-}$ MEFs were incubated with the autophagy inducers etoposide, ceramide, serum-free medium, EBSS, or vinblastine for 20 h. Afterward, the cells were double labeled with annexin V and propidium iodide (PI) and were analyzed by FACS. The results obtained in a typical experiment of EBSS induction are reported in Fig. 9 (A–D). The histogram presented in Fig. 9 E summarizes the results of four independent experiments for each specific stimulus. A dramatic increase in apoptosis can be seen in calpain-deficient cells after induction with all of the stimuli, with the exception of vinblastine. Vinblastine is a microtubule-depolymerizing agent, and, although it can trigger an autophagic response, it has inhibitory functions on late autophagic events (Punnonen and Reunanen, 1990). Interestingly, we have previously reported that the toxicity of taxol, an indirect inhibitor of autophagy by virtue of its block of microtubule depolymerization, is almost comparable in wild-type and CAPNS1$^{-/-}$ MEFS (Demarchi et al., 2005). Collectively, the aforementioned data highlight the cytoprotective potential of autophagy in MEFs and strongly argue for a strict correlation between the impairment of autophagy in calpain-deficient cells and induction of the apoptotic switch.

To further confirm this hypothesis, a similar approach was followed using human U2OS cells silenced either with *ATG5*, CAPNS1-specific siRNA, or a combination of the two. 48 h after silencing, the cells were shifted to amino acid–free medium and incubated for a further 20 h to trigger autophagy. Cell death was then quantified by means of PI and annexin staining followed by FACS analysis. Fig. 10 (A–F) presents the results of a representative experiment and indicates that both *ATG5* and CAPNS1 silencing sensitize U2OS cells to apoptosis induced by amino acid starvation. The mean values obtained in four independent experiments are reported in Fig. 10 G. The effect of CAPNS1 silencing is the most severe, suggesting that CAPNS1 depletion in addition to the block of autophagy also prevents other antiapoptotic mechanisms such as NF-κB activation (Demarchi et al., 2005).

Discussion

In this study, we demonstrate that calpain regulates macroautophagy in two cellular systems lacking calpain activity: MEFs derived from CAPNS1 knockout mice and CAPNS1-silenced

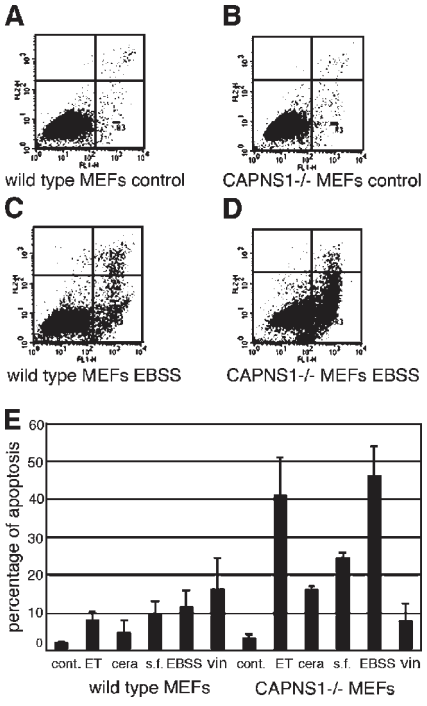

Figure 9. **CAPNS1$^{-/-}$ MEFs are more sensitive to apoptosis.** (A–D) Wild-type and CAPNS1$^{-/-}$ MEFs were treated with etoposide (ET), ceramide (cera), EBSS, serum-free medium (sf), and vinblastine (vin) or left in control medium (cont) for 20 h and stained with PI and annexin V–FITC. A set of representative experiments with EBSS is shown. The cells in the bottom right quadrant were scored as apoptotic. (E) The mean values obtained in four independent experiments with all of the stimuli. Error bars represent SD.

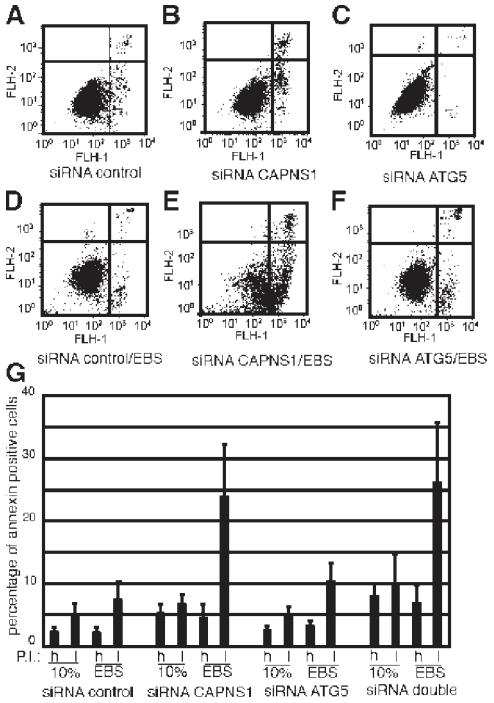

Figure 10. **Depletion of CAPNS1 results in increased apoptosis in human cells.** U2OS cells were transfected with a siRNA specific for CAPNS1, *ATG5*, or a combination of the two. An ineffective siRNA was used as a negative control. 48 h later, the cells were shifted to amino acid–free medium for an additional 20 h, stained with PI and annexin-FITC, and analyzed by FACS. (A–F) Results of a set of representative experiments. (G) The mean of the values obtained in four independent experiments. Bars indicate the percentage of annexin-positive cells with high (h) PI staining (top right quadrant in A–F) and low (l) PI staining (bottom right quadrant in A–F). Error bars represent SEM.

human cells. In addition, we shed some light on the relationship between apoptosis and autophagy.

Calpains are activated by several stimuli that trigger macroautophagy, including starvation (Gomez-Vicente et al., 2005), ceramide (Tanabe et al., 1998; Demarchi et al., 2005), etoposide (Varghese et al., 2001), and arsenic trioxide (Karlsson et al., 2004). Milli- and microcalpain, which both require CAPNS1 for activity, are localized at the endoplasmic reticulum and Golgi, where the autophagic machinery works (Kihara et al., 2001; Pattingre et al., 2005).

In both calpain-null systems used in this study, deficient autophagy was shown by four different approaches: analysis of exogenous and endogenous LC3 by immunofluorescence and Western blotting, quantification of lysosomal induction, long-lived protein degradation assays, and electron microscopy. Altogether, the data presented indicate that in CAPNS1-deficient cells, the autophagic program is not efficiently activated. As a result of this defect, CAPNS1-deficient cells are more sensitive to apoptosis induced by several autophagic stimuli, including ceramide, etoposide, and starvation.

In light of our findings connecting calpain and autophagy, it will be interesting to investigate this relationship in vivo under physiological and pathological conditions as well as in response to chemotherapy. Previously reported data lend support to such a possibility. The dual role of autophagy has been seen during cancer progression, where, at the initial stages, autophagy prevents tumor growth (Liang et al., 1999), whereas at advanced stages, it might favor tumor cell survival (Paglin et al., 2001). An example of this is calpain 9, which appears to be a tumor suppressor of gastric cancer, whereas calpain activation has been shown to be involved in cell transformation and invasion (Carragher and Frame, 2002; Xu and Deng, 2004).

Most interestingly, this parallel is maintained in other degenerative pathologies. Autophagy is protective during the initial stages of neurodegeneration (Webb et al., 2003; Ravikumar et al., 2004), whereas it becomes deleterious at later stages (Yue et al., 2002). A similar dual role could be played by calpain in neuronal diseases, where it may be protective at the initial stages of neurodegeneration (Kim et al., 2003) and hyperactivated and detrimental at advanced stages (Park and Ferreira, 2005). A detailed investigation of the molecular cross talk between these two systems in living organisms might be instrumental for performing appropriate strategies of molecular intervention.

The precise molecular network linking autophagy, apoptosis, and other types of cell death is still unresolved (Assuncao Guimaraes and Linden, 2004; Kroemer and Jaattela, 2005). Autophagy is protective against low radiation damage (Paglin et al., 2001) and against mutant huntingtin-induced cell death (Bjorkoy et al., 2005); it is essential for maintaining cell survival after growth factor withdrawal in $Bax^{-/-}Bak^{-/-}$ cells (Lum et al., 2005). Furthermore, the inhibition of macroautophagy triggers apoptosis (Boya et al., 2005; Gonzalez-Polo et al., 2005). On the other hand, autophagy is coupled to cell death in $Bax^{-/-}Bak^{-/-}$ MEFs (Shimizu et al., 2004) and in tamoxifen-treated MCF7 cells (Bursch et al., 2000). In addition, autophagy and apoptosis are positively interconnected in several systems, including *Drosophila* development (Baehrecke, 2003), rat retinal tissue development (Guimaraes et al., 2003), and peripheral nerves of adult rats after damage (Xue et al., 1999). Collectively, our data further support the argument that macroautophagy is a survival strategy activated both in response to serum and amino acid deprivation. In addition, we have shown that macroautophagy is activated and also plays a protective role upon treatment with specific drugs, such as etoposide and ceramide; thus, the knockdown of autophagy could be a strategy for improving chemotherapy protocols.

Ectopic LC3 is a powerful tool to study autophagy (Kabeya et al., 2000). In this study, we confirmed that in MEFs and U2OS human osteosarcoma cells, the formation of LC3 autophagosomes is efficiently inhibited by treatment with the autophagy inhibitor 3MA and by siRNA-mediated depletion of the essential autophagy gene *ATG5*, respectively. However, in $CAPNS1^{-/-}$ MEFs and siCAPNS1-depleted cells, we observed that ectopic LC3 constitutively accumulates in the absence of any specific autophagic stimulus into cytoplasmic endosome-like bodies enriched with endosomal markers. Therefore, we hypothesize that such LC3 bodies could represent a default or salvage lysosomal pathway for protein degradation with slower clearance kinetics, which becomes manifest in a calpain-deficient cellular context. A similar pathway may be predicted for the endogenous proteins that accumulate in diseases coupled to autophagy defects.

Further studies are required to analyze the detailed mechanisms involving calpains in the formation of autophagosomes and in lysosomal-mediated protein degradation pathways. Given the strategic localization of milli- and microcalpain at the endoplasmic reticulum, it would be tempting to speculate that calpain may play a role in the delivery of membranes to the autophagosome. Alternatively, calpain could modulate one or more key components of the signaling networks, ultimately leading to autophagosome formation. The complete block of autophagosome formation occurring in rapamycin-treated CAPNS1$^{-/-}$ MEFs favors such a possibility.

Materials and methods

Chemicals and reagents
C2 ceramide, bafilomycin, pepstatin A, 3MA, rapamycin, and etoposide were purchased from Sigma-Aldrich. LipofectAMINE reagent and Oligofectamine were purchased from Invitrogen. SMARTpool for CAPNS1 silencing was obtained from Dharmacon. Micro- and millicalpain siRNAs were purchased from Santa Cruz Biotechnology, Inc.

Plasmids and constructs
HcRed-hLC3 and pGFP-hLC3 were constructed by inserting human LC3 in HcRed and pGFP plasmid, respectively. The plasmid pGFP-rLC3 was a gift from T. Yoshimori (National Institute of Genetics, Shizuoka, Japan). The plasmid siCapns1-GFP was obtained by subcloning a double-stranded oligonucleotide containing a sequence complementary to CAPNS1 siRNA into commercial p-superior–GFP plasmid according to the manufacturer's instructions. All constructs were checked by sequence analysis.

Cell culture
Wild-type and CAPNS1$^{-/-}$ MEFs (Dourdin et al., 2001) were gifts from P.A. Greer (Queen's University, Kingston, Ontario, Canada). U2OS cells and the aforementioned mouse fibroblasts were grown in DME supplemented with 10% FCS.

Immunological procedures and quantifications
Standard protocols for immunoblotting and immunofluorescence were used. Rabbit serum raised against LC3 was provided by T. Yoshimori. Monoclonal antibody against LAMP-2 was purchased from BD Biosciences. LAMP-1–specific antibody was purchased from Santa Cruz Biotechnology, Inc., and monoclonal anti-CAPNS1 was purchased from Sigma-Aldrich. Monoclonal antitransferrin receptor (OKT9) was previously described (Sutherland et al., 1981). Band quantification from Western blots was performed using the Image 1.63.sea program (Scion). Secondary antibodies for immunofluorescence were FITC conjugated, and the cells were mounted using Mowiol medium. Analysis and acquisition were performed using a confocal laser-scanning microscope (Axiovert 100 M; Carl Zeiss MicroImaging, Inc.) with a 63× NA 1.25 or 100× NA 1.30 oil objective (Leica) at room temperature. Images were imported using LSM-510 software (Carl Zeiss MicroImaging, Inc.). ImageJ software (National Institutes of Health) was used to quantify the colocalization observed by immunofluorescence.

Transfection
Stable transfections of U2OS cells with HcRed-LC3 were performed by the calcium phosphate method using standard procedures. U2OS, CAPNS1$^{-/-}$, and control mouse fibroblasts at 60–80% confluency were transiently transfected or oligofected using FuGene (Roche) or Oligofectamine (Life Technologies) according to the manufacturer's instructions.

Statistical analysis
Results are expressed as means ± SD of at least three independent experiments performed in triplicate or quadruplicate unless indicated otherwise. Statistical analysis was performed using a *t* test, with the level of significance set at $P < 0.05$.

LysoTracker labeling and quantification
To label lysosomes, LysoTracker green (Invitrogen) was used at a final concentration of 75 nM. The cells induced for 3 or 24 h with the stimuli were trypsinized, resuspended in phenol-free DME, 10% FCS, and 75 nM LysoTracker green, incubated for 30 min at 37°C, and analyzed with the CellQuest program (BD Biosciences) by FacsCalibur (Becton Dickinson).

Protein degradation assay
Cells were labeled in complete medium in the presence of [^{14}C]valine for 18 h, washed, and incubated with cold medium for 1 h to allow the degradation of short-lived proteins. Then, after extensive washing, the medium was replaced with EBSS for 4 h in the presence or absence of 10 mM 3MA. Finally, the proteins were precipitated with TCA, and radioactivity was measured. Protein degradation was calculated as the percentage of TCA-soluble counts on total radioactivity.

Electron microscopy
Monolayers were fixed in 2% glutaraldehyde in 0.2 M Hepes, pH 7.4, for 2 h and were scraped off the dish during fixation. The pellets were embedded in Epon using routine procedures. Approximately 60-nm sections were cut and stained using uranyl acetate and lead citrate and were examined with an electron microscope (JEM 1200EXII; JEOL). The number of AVi and AVd profiles was counted under the microscope by systematically screening the sections at 12,000× using grid squares as sampling units, as previously described (Eskelinen et al., 2004).

All AVs occurring in the grid were recorded. The area of cells on each grid square was estimated by point counting using photographic negatives taken at 600×. Four to five grid squares were screened for each sample. The number of vacuoles per cell area was then counted for each grid square separately.

For immunogold electron microscopy, U2OS cells were fixed in 4% PFA in 0.2 M Hepes, pH 7.4, for 2 h at room temperature and were further processed as previously described (Eskelinen et al., 2002). The cell sections were analyzed by immunogold electron microscopy with rabbit anti-GFP and mouse anti–LAMP-2 antibodies followed by the secondary antibodies goat anti–rabbit conjugated to 10 nm gold and goat anti–mouse coupled to 5 nm gold.

Annexin V and PI staining and FACS analysis
Translocation of phosphatidylserine to the cell surface was monitored by using an annexin V–FITC apoptosis detection kit (Sigma-Aldrich). Cells were trypsinized, washed in PBS, and resuspended in binding buffer (10 mM Hepes/NaOH, pH 7.4, 140 mM NaCl, and 2.5 mM $CaCl_2$). Cell density was adjusted to 2–5 × 10^5 cells/ml. 1 μl of recombinant human annexin V–FITC/a and 2 μl PI were added to 100 μl of cell suspension; the mixture was briefly mixed and incubated for 10 min at room temperature in the dark. Afterward, 400 μl of binding buffer was added to the cells that were then analyzed by FACScan (Becton Dickinson). 15,000 events were collected in list mode fashion, stored, and analyzed by CellQuest software (BD Biosciences).

Online supplemental material
Fig. S1 shows that the depletion of microcalpain impairs macroautophagy. Fig. S2 shows that the fine ultrastructure of autophagosomes is not altered in CAPNS1$^{-/-}$ MEFs. Fig. S3 shows that rapamycin inhibits Tor activity in wild-type and CAPNS1$^{-/-}$ MEFs. Fig. S4 shows that LC3II is associated with membranes in CAPNS1$^{-/-}$ MEFs. Fig. S5 shows that the induction of LysoTracker-labeled bodies is reduced in CAPNS1$^{-/-}$ MEFs. Online supplemental material is available at http://www.jcb.org/cgi/content/full/jcb.200601024/DC1.

We are grateful to Stefania Marzinotto for technical support, Peter Greer for providing CAPNS1$^{-/-}$ (calpain 4$^{-/-}$) MEFs, and Tamotzu Yoshimori for the gifts of anti-LC3 antibody and GFP-rLC3 plasmid. We thank Francesca Scarlatti (S. Paolo Medical School, Milan, Italy) and Patrice Codogno (Institut National de la Santé et de la Recherche Médicale, Villejuif, France) for providing protocols and useful suggestions and Georgine Faulkner (The International Centre for Genetic Engineering and Biotechnology [ICGEB], Trieste, Italy) for critically revising the manuscript. We are grateful to Mauro Giacca (ICGEB) for access to FACS and the confocal microscope.

This work was supported by grants AIRC 1214, MIUR FIRB2001, and MIUR PRIN2004 to C. Schneider. C. Bertoli is a recipient of a fellowship from FIRC. T. Copetti is a student at the International School for Advanced Studies (Trieste, Italy).

Submitted: 5 January 2006
Accepted: 13 October 2006

References

Arthur, J.S., J.S. Elce, C. Hegadorn, K. Williams, and P.A. Greer. 2000. Disruption of the murine calpain small subunit gene, Capn4: calpain is essential for embryonic development but not for cell growth and division. *Mol. Cell. Biol.* 20:4474–4481.

Assuncao Guimaraes, C., and R. Linden. 2004. Programmed cell deaths. Apoptosis and alternative deathstyles. *Eur. J. Biochem.* 271:1638–1650.

Baehrecke, E.H. 2003. Autophagic programmed cell death in *Drosophila*. *Cell Death Differ.* 10:940–945.

Benetti, R., G. Del Sal, M. Monte, G. Paroni, C. Brancolini, and C. Schneider. 2001. The death substrate Gas2 binds m-calpain and increases susceptibility to p53-dependent apoptosis. *EMBO J.* 20:2702–2714.

Bhatt, A., I. Kaverina, C. Otey, and A. Huttenlocher. 2002. Regulation of focal complex composition and disassembly by the calcium-dependent protease calpain. *J. Cell Sci.* 115:3415–3425.

Bjorkoy, G., T. Lamark, A. Brech, H. Outzen, M. Perander, A. Overvatn, H. Stenmark, and T. Johansen. 2005. p62/SQSTM1 forms protein aggregates degraded by autophagy and has a protective effect on huntingtin-induced cell death. *J. Cell Biol.* 171:603–614.

Boya, P., R.A. Gonzalez-Polo, N. Casares, J.L. Perfettini, P. Dessen, N. Larochette, D. Metivier, D. Meley, S. Souquere, T. Yoshimori, et al. 2005. Inhibition of macroautophagy triggers apoptosis. *Mol. Cell. Biol.* 25:1025–1040.

Bursch, W., K. Hochegger, L. Torok, B. Marian, A. Ellinger, and R.S. Hermann. 2000. Autophagic and apoptotic types of programmed cell death exhibit different fates of cytoskeletal filaments. *J. Cell Sci.* 113:1189–1198.

Camougrand, N., A. Grelaud-Coq, E. Marza, M. Priault, J.J. Bessoule, and S. Manon. 2003. The product of the UTH1 gene, required for Bax-induced cell death in yeast, is involved in the response to rapamycin. *Mol. Microbiol.* 47:495–506.

Carragher, N.O., and M.C. Frame. 2002. Calpain: a role in cell transformation and migration. *Int. J. Biochem. Cell Biol.* 34:1539–1543.

Demarchi, F., C. Bertoli, P.A. Greer, and C. Schneider. 2005. Ceramide triggers an NF-κB-dependent survival pathway through calpain. *Cell Death Differ.* 12:512–522.

Dewitt, S., and M.B. Hallett. 2002. Cytosolic free Ca(2+) changes and calpain activation are required for β integrin-accelerated phagocytosis by human neutrophils. *J. Cell Biol.* 159:181–189.

Dourdin, N., A.K. Bhatt, P. Dutt, P.A. Greer, C.H. Graham, J.S. Arthur, J.S. Elce, and A. Huttenlocher. 2001. Reduced cell migration and disruption of the actin cytoskeleton in calpain-deficient embryonic fibroblasts. *J. Biol. Chem.* 276:48382–48384.

Eskelinen, E.L., A.L. Illert, Y. Tanaka, G. Schwarzmann, J. Blanz, K. von Figura, and P. Saftig. 2002. Role of LAMP-2 in lysosome biogenesis and autophagy. *Mol. Biol. Cell*. 13:3355–3368.

Eskelinen, E.L., C.K. Schmidt, S. Neu, M. Willenborg, G. Fuertes, N. Salvador, Y. Tanaka, R. Lullmann-Raucht, D. Hartman, J. Heeren, et al. 2004. Disturbed cholesterol traffic but normal proteolytic function in LAMP-1/LAMP-2 double-deficient fibroblasts. *Mol. Biol. Cell*. 15:3132–3135.

Ghidoni, R., J.J. Houri, A. Giuliani, E. Ogier-Denis, E. Parolari, S. Botti, C. Bauvy, and P. Codogno. 1996. The metabolism of sphingo(glyco)lipids is correlated with the differentiation-dependent autophagic pathway in HT-29 cells. *Eur. J. Biochem.* 237:454–459.

Goll, D.E., V.F. Thompson, H. Li, W. Wei, and J. Cong. 2003. The calpain system. *Physiol. Rev.* 83:731–780.

Gomez-Vicente, V., M. Donovan, and T.G. Cotter. 2005. Multiple death pathways in retina-derived 661W cells following growth factor deprivation: crosstalk between caspases and calpains. *Cell Death Differ.* 12:796–804.

Gonzales-Polo, R.A., P. Boya, A.L. Pauleau, A. Jalil, N. Larochette, S. Souquere, E.L. Eskelinen, G. Pierron, P. Saftig, and G. Kroemer. 2005. The apoptosis/autophagy paradox: autophagic vacuolization before apoptotic death. *J. Cell Sci.* 118:3091–3102.

Guimaraes, C.A., M. Benchimol, G.P. Amarante-Mendes, and R. Linden. Alternative programs of cell death in developing retinal tissue. 2003. *J. Biol. Chem.* 278:41938–41946.

Hayashi, M., Y. Koshihara, H. Ishibashi, S. Yamamoto, S. Tsubuki, T.C. Saido, S. Kawashima, and M. Inomata. 2005. Involvement of calpain in osteoclastic bone resorption. *J. Biochem. (Tokyo)*. 137:331–338.

Hood, J.L., W.H. Brook, and T.L. Roszman. 2004. Differential compartmentalization of the calpain/calpastatin network with the endoplasmic reticulum and Golgi apparatus. *J. Biol. Chem.* 279:43126–43135.

Ichimura, Y., T. Kirisako, T. Takao, Y. Satomi, Y. Shimonishi, N. Ishihara, N. Mizushima, I. Tanida, E. Kominami, M. Ohsumi, et al. 2000. A ubiquitin-like system mediates protein lipidation. *Nature*. 408:488–492.

Kabeya, Y., N. Mizushima, T. Ueno, A. Yamamoto, T. Kirisako, T. Noda, E. Kominami, Y. Ohsumi, and T. Yoshimori. 2000. LC3, a mammalian homologue of yeast Apg8p, is localized in autophagosome membranes after processing. *EMBO J.* 19:5720–5728.

Kabeya, Y., N. Mizushima, A. Yamamoto, S. Oshitani-Okamoto, Y. Ohsumi, and T. Yoshimori. 2004. LC3, GABARAP and GATE16 localize to autophagosomal membrane depending on form-II formation. *J. Cell Sci.* 117:2805–2812.

Kanzawa, T., Y. Kondo, H. Ito, S. Kondo, and I. Germano. 2003. Induction of autophagic cell death in malignant glioma cells by arsenic trioxide. *Cancer Res.* 63:2103–2108.

Karlsson, J., I. Porn-Ares, and S. Pahlman. 2004. Arsenic trioxide-induced death of neuroblastoma cells involves activation of Bax and does not require p53. *Clin. Cancer Res.* 10:3179–3188.

Kihara, A., Y. Kabeya, Y. Ohsumi, and T. Yoshimori. 2001. Beclin-phosphatidylinositol 3-kinase complex functions at the trans-Golgi network. *EMBO Rep.* 2:330–335.

Kim, S.J., J.Y. Sung, J.W. Um, N. Hattori, Y. Mizuno, K. Tanaka, S.R. Paik, J. Kim, and K.C. Chung. 2003. Parkin cleaves intracellular alpha-synuclein inclusions via the activation of calpain. *J. Biol. Chem.* 278:41890–41899.

Klionsky, D.J. 2005. Autophagy. *Curr. Biol.* 15:R282–R283.

Klionsky, D.J., and Y. Ohsumi. 1999. Vacuolar import of proteins and organelles from the cytoplasm. *Annu. Rev. Cell Dev. Biol.* 15:1–32.

Kroemer, G., and M. Jaattela. 2005. Lysosomes and autophagy in cell death control. *Nat. Rev. Cancer*. 5:886–897.

Kuma, A., M. Hatano, M. Matsui, A. Yamamoto, H. Nakaya, T. Yoshimori, Y. Ohsumi, T. Tokuhisa, and N. Mizushima. 2004. The role of autophagy during the early neonatal starvation period. *Nature*. 432:1032–1036.

Lee, C.Y., C.R. Simon, C.T. Woodard, and E.H. Baehrecke. 2002. Genetic mechanism for the stage- and tissue-specific regulation of steroid triggered programmed cell death in *Drosophila*. *Dev. Biol.* 252:138–148.

Liang, X.H., S. Jackson, M. Seaman, K. Brown, B. Kempkes, H. Hibshoosh, and B. Levine. 1999. Induction of autophagy and inhibition of tumorigenesis by beclin 1. *Nature*. 402:672–676.

Lum, J.J., D.E. Bauer, M. Kong, M.H. Harris, C. Li, T. Lindsten, and C.B. Thompson. 2005. Growth factor regulation of autophagy and cell survival in the absence of apoptosis. *Cell*. 120:237–248.

Martin, D.N., and E.H. Baehrecke. 2004. Caspases function in autophagic programmed cell death in *Drosophila*. *Development*. 131:275–284.

Mizushima, N., A. Yamamoto, M. Hatano, Y. Kobayashi, Y. Kabeya, K. Suzuki, T. Tokuhisa, Y. Ohsumi, and T. Yoshimori. 2001. Dissection of autophagosome formation using Apg5-deficient mouse embryonic stem cells. *J. Cell Biol.* 152:657–668.

Mizushima, N., A. Yamamoto, M. Matsui, T. Yoshimori, and Y. Ohsumi. 2004. In vivo analysis of autophagy in response to nutrient starvation using transgenic mice expressing a fluorescent autophagosome marker. *Mol. Biol. Cell*. 15:1101–1111.

Neely, A.N., J.R. Cox, J.A. Fortney, C.M. Schworer, and G.E. Mortimore. 1977. Alterations of lysosomal size and density during rat liver perfusion. Suppression by insulin and amino acids. *J. Biol. Chem.* 252:6948–6954.

Noda, T., and Y. Ohsumi. 1998. Tor, a phosphatidylinositol kinase homologue, controls autophagy in yeast. *J. Biol. Chem.* 273:3963–3966.

Paglin, S., T. Hollister, T. Delohery, N. Hackett, M. McMahill, E. Sphicas, D. Domingo, and J. Yahalom. 2001. A novel response of cancer cells to radiation involves autophagy and formation of acidic vesicles. *Cancer Res.* 61:439–444.

Park, S.Y., and A. Ferreira. 2005. The generation of a 17 kDa neurotoxic fragment: an alternative mechanism by which tau mediates beta-amyloid-induced neurodegeneration. *J. Neurosci.* 25:5365–5375.

Pattingre, S., C. Bauvy, and P. Codogno. 2003. Amino acids interfere with the ERK1/2-dependent control of macroautophagy by controlling the activation of Raf-1 in human colon cancer HT-29 cells. *J. Biol. Chem.* 278:16667–16674.

Pattingre, S., A. Tassa, X. Qu, R. Garuti, X.H. Liang, N. Mizushima, M. Packer, M.D. Schneider, and B. Levine. 2005. Bcl-2 antiapoptotic proteins inhibit Beclin 1-dependent autophagy. *Cell*. 122:927–939.

Pfeifer, U. 1973. Cellular autophagy and cell atrophy in the rat liver during long-term starvation. A quantitative morphological study with regard to diurnal variations. *Virchows Arch. B Cell Pathol.* 12:195–211.

Punnonen, E.L., and H. Reunanen. 1990. Effects of vinblastine, leucine, and histidine, and 3-methyladenine on autophagy in Ehrlich ascites cells. *Exp. Mol. Pathol.* 52:87–97.

Ravikumar, B., C. Vacher, Z. Berger, J.E. Davies, S. Luo, L.G. Oroz, F. Scaravilli, D.F. Easton, R. Duden, C.J. O'Kane, and D.C. Rubinsztein. 2004. Inhibition of mTOR induces autophagy and reduces toxicity of polyglutamine expansions in fly and mouse models of Huntington disease. *Nat. Genet.* 36:585–595.

Rusten, T.E., K. Lindmo, G. Juhasz, M. Sass, P.O. Seglen, A. Brech, and H. Stenmark. 2004. Programmed autophagy in the *Drosophila* fat body is induced by ecdysone through regulation of the PI3K pathway. *Dev. Cell*. 7:179–192.

Scarlatti, F., C. Bauvy, A. Ventruti, G. Sala, F. Cluzeaud, A. Vandewalle, R. Ghidoni, and P. Codogno. 2004. Ceramide-mediated macroautophagy involves inhibition of protein kinase B and up-regulation of beclin 1. *J. Biol. Chem.* 279:18384–18391.

Schad, E., A. Farkas, G. Jekely, P. Tompa, and P. Friedrich. 2002. A novel human small subunit of calpains. *Biochem. J.* 362:383–388.

Shimizu, S., T. Kanaseki, N. Mizushima, T. Mizuta, S. Arakawa-Kobayashi, C.B. Thompson, and Y. Tsujimoto. 2004. Role of Bcl-2 family proteins in a non-apoptotic programmed cell death dependent on autophagy genes. *Nat. Cell Biol.* 6:1221–1228.

Sutherland, R., D. Delia, C. Schneider, R. Newman, J. Kemshead, and M. Greaves. 1981. Ubiquitous cell-surface glycoprotein on tumor cells is proliferation-associated receptor for transferring. *Proc. Natl. Acad. Sci. USA*. 78:4515–4519.

Takacs-Vellai, K., T. Vellai, A. Puoti, M. Passannante, C. Wicky, A. Streit, A.L. Kovacs, and F. Muller. 2005. Inactivation of the autophagy gene bec-1 triggers apoptotic cell death in *C. elegans*. *Curr. Biol.* 15:1513–1517.

Tanabe, F., S.H. Cui, and M. Ito. 1998. Ceramide promotes calpain-mediated proteolysis of protein kinase C beta in murine polymorphonuclear leukocytes. *Biochem. Biophys. Res. Commun.* 242:129–133.

Varghese, J., G. Radhika, and A. Sarin. 2001. The role of calpain in caspase activation during etoposide induced apoptosis in T cells. *Eur. J. Immunol.* 31:2035–2041.

Webb, J.L., B. Ravikumar, J. Atkins, J.N. Skepper, and D.C. Rubinsztein. 2003. Alpha-Synuclein is degraded by both autophagy and the proteasome. *J. Biol. Chem.* 278:25009–25013.

Xu, L., and X. Deng. 2004. Tobacco-specific nitrosamine 4-(methylnitrosamino)-1-(3-pyridyl)-1-butanone induces phosphorylation of mu- and m-calpain in association with increased secretion, cell migration, and invasion. *J. Biol. Chem.* 279:53683–53690.

Xue, L., G.C. Fletcher, and A.M. Tolkovsky. 1999. Autophagy is activated by apoptotic signalling in sympathetic neurons: an alternative mechanism of death execution. *Mol. Cell. Neurosci.* 14:180–198.

Yorimitsu, T., and D.J. Klionsky. 2005. Autophagy: molecular machinery for self-eating. *Cell Death Differ.* 12:1542–1552.

Yu, L., A. Alva, H. Su, P. Dutt, E. Freundt, S. Welsh, E.H. Baehrecke, and M.J. Lenardo. 2004. Regulation of an ATG7-beclin 1 program of autophagic cell death by caspase-8. *Science*. 304:1500–1502.

Yue, Z., A. Horton, M. Bravin, P.L. DeJager, F. Selimi, and N. Heintz. 2002. A novel protein complex linking the delta 2 glutamate receptor and autophagy: implications for neurodegeneration in lurcher mice. *Neuron*. 35:921–933.

Yue, Z., S. Jin, C. Yang, A.J. Levine, and N. Heintz. 2003. Beclin 1, an autophagy gene essential for early embryonic development, is a haploinsufficient tumor suppressor. *Proc. Natl. Acad. Sci. USA*. 100:15077–15082.